Atmospheric Pollution Research

www.atmospolres.com

Monitoring the transport of biomass burning emission in South America

Gabriel Pereira [1], Yosio E. Shimabukuro [1], Elisabete C. Moraes [1], Saulo R. Freitas [2], Francielle S. Cardozo [1], Karla M. Longo [3]

[1] *Remote Sensing Division, National Institute for Space Research – INPE, Av. dos Astronautas, CEP 12227–010 – São José dos Campos – SP, Brazil.*
[2] *Center for Weather Forecasting and Climate Studies, National Institute for Space Research – INPE, Av. dos Astronautas, CEP 12227–010 – São José dos Campos – SP, Brazil.*
[3] *Center for Space and Atmospheric Sciences, National Institute for Space Research – INPE, Av. dos Astronautas, CEP 12227–010 – São José dos Campos – SP, Brazil.*

ABSTRACT

The main objective of this work is to use Fire Radiative Power (FRP) to estimate particulate matter with diameter less than 2.5 µm ($PM_{2.5}$) and carbon monoxide (CO) emissions for the South America 2002 burning season. Sixteen small–scale combustion experiments were performed near the Laboratory of Radiometry (LARAD) at the National Institute for Space Research (DSR/INPE) to obtain the coefficient that relates the biomass consumption with the FRP released. The fire products MOD14/MYD14 from the MODIS Terra/Aqua platforms and the Wildfire Automated Biomass Burning Algorithm (WFABBA) on the Geostationary Operational Environmental Satellite (GOES) were utilized to calculate the total amount of biomass burned. This inventory is modeled in the Coupled Chemistry–Aerosol–Tracer Transport model coupled to the Brazilian developments on the Regional Atmospheric Modeling System (CCATT–BRAMS) and compared with data collected in the Large Scale Biosphere–Atmosphere (LBA) Smoke, Aerosols, Clouds, rainfall, and Climate (SMOCC) and Radiation, Cloud, and Climate Interactions (RaCCI) Experiments. The relationship between the modeled $PM_{2.5}$ and CO shows a good agreement with SMOCC/RaCCI data in the general pattern of temporal evolution. The results showed high correlations, with values between 0.80 and 0.95 (significant at 0.05 level by student t–test), for the CCATT–BRAMS simulations with $PM_{2.5}$ and CO. Furthermore, the slope analysis reveals an underestimation of emission values with CCATT–BRAMS modeled values, 20–30% lower than observed data with discrepancies mainly on days with large fires. However, the underestimation is similar to the uncertainties in traditional emissions methods.

Keywords:
Biomass burned coefficient
Aerosol and trace gases emission
Fire radiative energy

Article History:
Received: 02 September 2010
Revised: 04 November 2010
Accepted: 07 December 2010

Corresponding Author:
Gabriel Pereira
Tel: +55-12-3208-6668
Fax: +55-12-3208-6488
E-mail: gabriel@dsr.inpe.br

doi: 10.5094/APR.2011.031

1. Introduction

In the pre–industrial period, the main sources of air pollution originated from plant and animal respiration, natural burnings and in a smaller scale from anthropogenic fires. Nowadays, biomass burning devastates large areas of forest and grassland, consuming large amounts of biomass and releasing an unknown amount of trace gases and aerosols into the atmosphere (Andreae and Merlet, 2001).

The biomass burning leads to variations in environmental characteristics, such as soil depletion, flora and fauna biodiversity reduction, as well as changes in biogeochemical cycles, global climate and atmospheric chemistry (Andreae et al., 2004; Moraes et al., 2005). The consequence of these effects have been assessed in several studies, such as on radiative balance (Christopher et al., 1998; Tarasova et al., 2000; Wagner et al., 2001; Moraes et al., 2005; Satheesh and Moorthy, 2005; Tzanis and Varotsos, 2008), on atmospheric chemistry (Crutzen and Andreae, 1990; Fishman et al., 1996; Panchenko et al., 2008), on the greenhouse emissions (Wooster, 2002; Dyominov and Zadorozhny, 2008; Pereira et al., 2009), and indirectly, on the reduction of evaporation and precipitation on the climate impacts (Nobre et al., 1998; Latifovic and Pouliot, 2007).

In the atmosphere, the aerosols from biomass burning lead to a direct radiative effect, related to the spectral absorption and scattering of solar radiation. They also lead to indirect effects, related to the action of these aerosols such as condensation nuclei modifying the optical properties of clouds. This modification, results in the change of cloud reflectivity of solar electromagnetic radiation (Kaufman and Fraser, 1997; Reid et al., 1999). On the surface, the changes of physical–chemical and biological properties by the action of fires are related to the reflected irradiance, an indirect measure of absorbed solar energy directly related to surface energy exchange (Pereira et al., 2000; Liang, 2001).

In South America, temporal and spatial variability in land–use and land–cover due to agricultural land clearing, grassland management and deforestation of the Amazon tropical rainforest contribute to variations in anthropogenic biomass burning (Kaufman et al., 1990; Kaufman et al., 1992; Ward et al., 1992; van der Werf et al., 2006). The South America continent is one of the regions that might contribute to aerosols and trace gas emissions associated with land–use and has a great potential for future emissions from the large remaining areas of tropical forest (Fearnside et al., 2009).

The traditional emission methods for estimating aerosols and trace gases commonly utilize emission factors associated with burned dry mass and fuel load characteristics (Andreae and Merlet, 2001). However, while emission factors for different species and biomes are accurately determined, other features such as burned area and burning efficiency (Chuvieco et al., 2004) are usually

accessible only a long time after the fire is over (Roy et al., 2002; Silva et al., 2005). Recently, new methods have been developed to derive the burned biomass and fire emissions from environmental satellite Fire Radiative Power (FRP) measurements (Wooster, 2002; Wooster et al., 2003; Ichoku and Kaufman, 2005; Pereira et al., 2009). In theory, radiative intensity released by fires is linearly correlated with burned biomass and might be independent of vegetation type (Wooster et al., 2005; Freeborn et al., 2008).

An advantage of methods that utilize the FRP to estimate the biomass burning emissions is the possibility of near real–time assimilation in chemistry transport models (Chatfield et al., 2002; Horowitz et al., 2003; Freitas et al., 2009). An example of fire emissions coupled to an atmospheric model is the European Centre for Medium–Range Weather Forecasts (ECMWF) Monitoring Atmospheric Composition and Climate (MACC) system that derives biomass burning emissions from Spinning Enhanced Visible and Infra–red Imager (SEVIRI) and MODIS fire products (Kaiser et al., 2009).

However, FRP–based emission coefficients must be evaluated with ground data to verify the agreement of satellite emission retrievals. In this study, sixteen small–scale combustion experiments using Brazilian grassland were performed to create an FRP–based coefficient to estimate the biomass burned. The coefficient originated in the Laboratory of Radiometry (LARAD) of the National Institute for Space Research (INPE) is also used in simulations with the Coupled Chemistry–Aerosol–Tracer Transport Model coupled to the Brazilian developments on the Regional Atmospheric Modeling System (CCATT–BRAMS). The results are then assessed with field campaign data collected in the Large Scale Biosphere–Atmosphere in Amazonia (LBA) Smoke, Aerosols, Clouds, Rainfall, and Climate (SMOCC) and Radiation, Cloud, and Climate Interactions (RaCCI) (Andreae et al., 2004; Freitas et al., 2009).

2. Materials and Methods

2.1. Fire radiative power

The fraction of chemical energy emitted from biomass burning as electromagnetic radiation can be defined as FRP (in MJ s^{-1}), and the temporal integration of FRP gives the Fire Radiative Energy (FRE, in MJ). Initial studies with FRP were performed with the MODIS Airborne Simulator (MAS) in the SCAR–C and SCAR–B (Smoke, Cloud and Radiation – California/Brazil) experiments (Kaufman et al., 1998). FRP is available from the MODIS fire products, also known as MOD14 (Terra) and MYD14 (Aqua), utilizing a contextual algorithm applied to brightness temperatures in the 4 µm and 11 µm infrared radiation channels. They use red and near–infrared channels to avoid false alarms and mask clouds (Justice et al., 2002; Giglio, 2005). The FRP is calculated for each fire pixel through the method proposed by Kaufman et al. (1996, 1998).

Moreover, while MODIS gives information of active fires 4 to 5 times per day for a given area, the WFABBA fire product, based on GOES observations, is available for South America with a higher observation frequency, approximately 48 times per day. GOES's retrieve regional–scale FRE release rate capability was assessed by Pereira et al. (2009), showing a correlation greater than 96% between monthly FRP measurements derived from these two sensors (significant at 0.05 level by student t–test), with a ratio of 0.34 between MODIS and GOES FRP. This difference could be explained by instrument characteristics such as radiometric, spectral and spatial resolutions, sensor noise, sensor point spread function (PSF) and atmospheric transmittance. Consequently, this proportion was used to normalize MODIS and GOES FRP measurements.

To perform the FRP estimation of saturated pixel in WFABBA/GOES fire product, an alternative approach was adopted to assimilate FRP–based burned biomass inventory into the CATT–BRAMS model. We used the middle infrared (MIR) radiance method proposed by Wooster et al. (2003) applied to WFABBA data, with a constant background temperature of 300 K. The MIR radiance method for FRP estimation is based on the assumption that spectral radiance emitted in 3.9 µm waveband is linearly proportional to the FRP. The MIR radiance method approach is expressed by:

$$FRP_{MIR} = \frac{Ag}{a}\sigma \int_{3.76}^{4.03} B(\lambda,T)d\lambda - L_b$$
$$B(\lambda,T) = \frac{c_1}{\lambda^5(\exp(\frac{c_2}{\lambda T})-1)} \quad (1)$$

where *Ag* is GOES pixel area (16 km²); *a* is a constant fit based on GOES MIR spectral channel (3.07; 3.06 or 3.08 x10^{-9} W m^{-2} sr^{-1} µm^{-1} K^{-4}, to GOES–8, GOES–9/10 and GOES–12 imager, respectively) acquired from Wooster et al. (2005); *B(λ,T)* is Planck's Radiation law; c_1 and c_2 are constants (3.74x10^8 W m^{-2} and 1.44x10^4 µm K, respectively); λ is wavelength (µm); T is temperature (K) and L_b (W m^{-2} sr^{-1} µm^{-1}) is the spectral radiance emitted by adjacent pixel. In this work, we adopted as surround background contribution in FRP estimation a value of 110 MW.

2.2. Experiments setup

Sixteen biomass combustion experiments were performed in the LARAD/INPE during the night to minimize the influence of solar radiation over the collected signal. Dead fuels were utilized to simulate the conditions found during the South America fire season. The primary fuel was *Brachiaria sp.* (*Cyperales: Poaceae*), a tall perennial grass from the Brazilian "Cerrado" used in 13 burned samples; the other species was *Stenotaphrum sp.* (*Polaes: Poaceae*), used in 3 experiments. Both fuel types were dried to a gravimetric moisture content of approximately 30%.

Figure 1 shows the biomass combustion experiment setup in which a 4.0 m structure (a) was placed. The spectrometer FieldSpec Pro FR (b), located at a distance of 1.1 m and 2.6 m from the biomass samples, measured the radiance released in the combustion process. The fuel bed was filled with sand to a 3 cm depth (c), covered with biomass which filled completely the spectrometer's instantaneous field–of–view (IFOV), and positioned on a scale (d) with a 0.1 kg precision. The sample weight was measured at intervals of 10 seconds showing the total amount of biomass consumed over the time. In the combustion experiments, initial fuel mass varied from 0.40–1.15 kg. The spectroradiometer FieldSpec Pro FR provided measurement of the fires spectral radiance ranging from 350 to 2 500 nm with a 25° field of view, a spectral resolution of 3 to 10 nm and time acquisition of 0.1 second per sample.

The FieldSpec Pro FR records data as raw digital numbers, which are converted into spectral radiance by applying the calibration parameters specific to each device. Also, an optimization is performed before each radiance measurement to normalize the signal collected from 3 sets of detectors array, a silicon photodiode (350–1 000 nm) and two Indium–Gallium–Arsenide (900–1 850 nm; 1 700–2 500 nm) sets (Biggar et al., 1994; Starks et al., 1995).

The FieldSpec spectroradiometer radiance measurements can be represented by ratio of output radiant flux (ϕ) per solid angle (θ), cosine of zenith angle (θ) and the area (*A*), as shown in Equation (2).

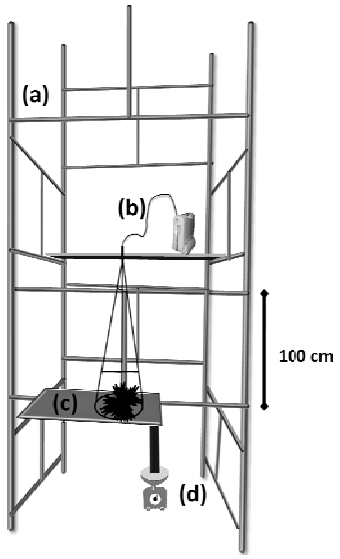

Figure 1. *Design and position of the field experiment equipment.*

$$L = \frac{\partial \phi}{\partial \omega \; cos\theta \; \partial A} \quad (\text{W m}^{-2}\ \text{sr}^{-1}\ \mu\text{m}^{-1}) \tag{2}$$

However, the spectroradiometer utilized in the experiment is a field unit and must be calibrated with a standard laboratorial spectroradiometer. The spectral radiance measurements are corrected using an ideal lambertian plate (*Lip*) with laboratorial use only and a calibrated unit. The same observation (θ) and acquisition characteristics (ϕ) were used for the calibration.

$$L_{(\lambda,\theta_i,\phi_i,\theta_o,\phi_o)} = L_{field\ unit} \cdot \frac{Lip_{(\lambda,\theta_i,\phi_i,\theta_o,\phi_o,Field\,Unit)}}{Lip_{(\lambda,\theta_i,\phi_i,\theta_o,\phi_o,Calibrated\,Unit)}} \tag{3}$$

Although the spectroradiometer used in combustion experiments does not cover the mid–infrared electromagnetic region, Wooster et al. (2003) showed a good agreement between the FRE release rate derived by the MIR AGEMA 550 Camera and by spectroradiometer GER 3700, allowing the use of this method to estimate burned biomass coefficient. In combustion experiments, FRP are estimated from each radiance spectrum collected by the spectroradiometer through the similarity with the curve of a temperature emitter given by Planck´s Radiation Law as described in Wooster et al. (2003).

2.3. Model description

The CATT, an Eulerian transport model fully coupled to BRAMS, is a numerical model that simulates biomass burning emissions, deposition and transport at grid and sub–grid scales. In this model, the trace gas and aerosol emissions, deposition and transport estimation are obtained simultaneously with the evolution of the atmospheric condition, using the dynamic and physical parameterizations of the atmospheric integration model. The mass continuity equation for CO and $PM_{2.5}$ in the form of a tendency equation is expressed as:

$$\frac{\partial \overline{s}}{\partial t} = \underbrace{\left(\frac{\partial \overline{s}}{\partial t}\right)_{\text{adv}}}_{\text{I}} + \underbrace{\left(\frac{\partial \overline{s}}{\partial t}\right)_{\text{PBL diff}}}_{\text{II}} + \underbrace{\left(\frac{\partial \overline{s}}{\partial t}\right)_{\text{deep conv}}}_{\text{III}} + \underbrace{\left(\frac{\partial \overline{s}}{\partial t}\right)_{\text{shallow conv}}}_{\text{IV}} + \underbrace{\left(\frac{\partial \overline{s}}{\partial t}\right)_{\text{chem CO}}}_{\text{V}} + \underbrace{W_{\text{PM}_{2.5\mu\text{m}}}}_{\text{VI}} + \underbrace{R}_{\text{VII}} + \underbrace{Q_{\text{pr}}}_{\text{VIII}} \tag{4}$$

where $\overline{s}$ is the grid box mean tracer mixing ratio; term (I) is the 3D transport (advection by mean wind); term (II) represents the sub–grid scale diffusion in the planetary boundary layer (PBL); terms (III) and (IV) are the sub–grid transport by deep and shallow convection, respectively; term (V) is applied to CO which is treated as a passive tracer with a 30–day lifetime (Seinfeld and Pandis, 1998); term (VI) is the wet removal applied to $PM_{2.5}$; term (VII) refers to the dry deposition applied to gases and aerosol particles and, finally term (VIII) is the source term that includes the plume rise mechanism associated with the vegetation fires (Freitas et al., 2007; Longo et al., 2010).

The model simulations for 17 July–14 November 2002 were performed with a 50 km horizontal resolution grid and represent the South America dry season. The vertical resolution varied telescopically with higher resolution at the surface (150 m) with a ratio of 1.07 up to a maximum vertical resolution of 850 m, with the top model altitude of 20 km at 38 vertical levels. CO and meteorological fields are initialized using horizontally homogeneous profiles associated with a background situation. The model was run for a period of 15 days with sources for the spin–up. Lateral boundary condition was defined as having constant inflow and radiative variable outflow. CO emissions from urban–industrial vehicular activities and biogenic sources are not included in this study because, in the areas where the model discussion was focused, biomass burning is the most important emission source.

The total time integration model lasted 124 days. For these days the initial atmosphere and boundary conditions were acquired from the European Center for Medium range Weather Forecasting (ECMWF) and from Center for Weather Forecasting and Climate Studies (CPTEC/INPE) models.

2.4. Source emission parameterization and evaluation with observed data

Spatial location and FRP estimation were extracted for every fire pixel detected by MODIS/EOS and GOES. In pre–processing step, all FRP values derived from both satellites are grouped in grid box of 16 km^2 and time integrated. Therefore, a land–use and land–cover map was used to extract the emission factors (Table 1). The 2002 South America dry season CO and $PM_{2.5}$ emission inventories are estimated by the integration of FRP over the lifetime of a detected fire (Figure 2), associated with emission factors (Andreae and Merlet, 2001) for each vegetation type and FRP–based biomass burned coefficient, as described in Equation (5).

$$Emission^{[\in]} = EF^{[\in]}\, BC \int FRP\ dt \tag{5}$$

where $EF^{[\in]}$ is the emission factor for a certain specie (in g kg^{-1}) and BC represents the biomass burned coefficient (in kg MJ^{-1}).

Table 1. *Average emission factors (EF) for $PM_{2.5}$ and CO (g kg^{-1}) used in CCATT-BRAMS model*

	Tropical Forest	Savanna	Pasture	Extra Tropical Forest	Cropland	Biofuel
CO	103.0	63.0	63.0	106.0	63.0	76.0
$PM_{2.5}$	9.1	4.9	4.9	13.0	4.9	5.7

The CATT–BRAMS model simulations of CO and $PM_{2.5}$ are compared with ground data from LBA SMOCC/RaCCI campaign, collected near 62.37°W and 10.75°S in the Amazon basin. The $PM_{2.5}$ and CO near–surface measurements were made at a pasture site in Ouro Preto do Oeste from September to November 2002. The $PM_{2.5}$ particle mass concentration is measured with a TEOM (Tapered Element Oscillation Microbalance) with a 30–min temporal resolution from 10 September to 4 November 2002.

Therefore, an intercomparison of the $PM_{2.5}$ and CO model results at 12:00 UTC with the daily average centered at 12:00 UTC is done to evaluate these simulations.

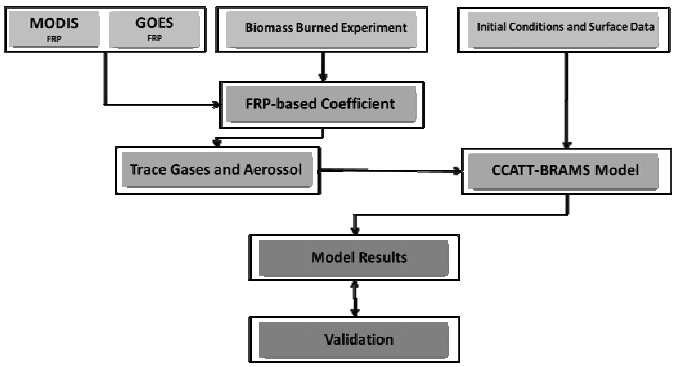

Figure 2. *Methodology flowchart.*

3. Results

3.1. Radiance released and biomass burned coefficient

In the combustion experiments, FRE released rate shows a notable relationship with total burned biomass. Figure 3 shows the temporal evolution of spectral radiance released in a small–scale combustion experiment with 0.65 kg of *Brachiaria*. Although the spectral curve represents a unique case, the other 15 samples submitted to the combustion process showed a similar response. They differ only by the intensity of FRE released and duration of each fire. A few seconds after fire ignition (3 seconds) the radiance released is near zero; this occurs because all the data acquisition took place at night. When the flames increase and cover all the IFOV area, the radiance shows high values in wavelengths greater than 2 300 nm. Twenty seconds after the fire ignition, the radiance values increased to near 150 W m^{-2} sr^{-1} μm^{-1}, for approximately 30 to 250 seconds these values remained near 200 W m^{-2} sr^{-1} μm^{-1}, and as soon as the flame phase finished the radiance released decreased to close to zero at the end of the experiment.

Figure 4a shows the relationship between the total FRE released in the sixteen combustion experiments, retrieved by the spectral radiance measurements, corresponding to the modeled emitter temperature blackbody curve derived from Planck´s Radiation Law, and total burned biomass. The linear regression with a 99% confidence interval (dashed line) shows a correlation of 0.86 (significant at 0.01 level by student t–test) between Biomass Burned (y–axis in kg) and FRE (x–axis in MJ). In this study, for each 1 kg of dry biomass of *Brachiaria*, approximately 1.8 MJ are released by fire. Figures 4b and 4c show the slope distributions and correlation using the bootstrap technique developed by Efron (1982) applied to the linear regression. In this method, a population of $1.0x10^4$ reconstructs the original curve and provides the parameters to create the confidence interval for the model estimate. As shown in Figures 4b and 4c, the common distribution values for slope are between 0.6 and 1.3, with a mean value centered at 1.0 with an error of approximately 10% in the coefficient found (significant at 0.05 by student t–test). Moreover, the highest frequencies of burned biomass correlation coefficient vary from 0.80 to 0.95.

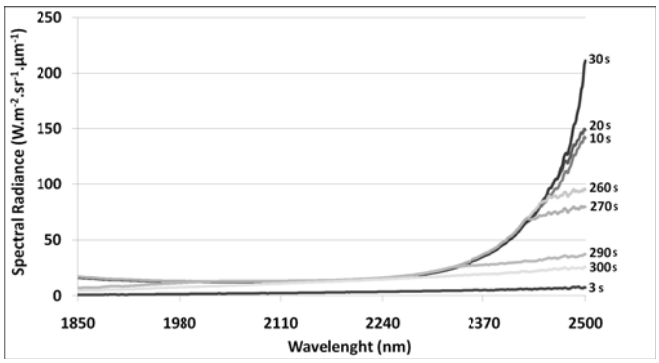

Figure 3. *Temporal evolution of the radiance released in 0.65 kg of burned biomass collected by the FieldSpec Pro FR between 3 and 300 seconds after fire ignition.*

The coefficient found in the small–scale combustion experiments, when applied by the FRE satellite measurements, gives the total biomass consumed, as described in Wooster et al. (2005). The relationship between burned biomass and FRE released can be expressed by Equation (6):

$$BC = 0.95 \int FRP\, dt \qquad (6)$$

where BC represents the biomass consumed (in kg) and FRE is the integrated Fire Radiative Power over the lifetime of a detected fire from MODIS and GOES data (in MJ).

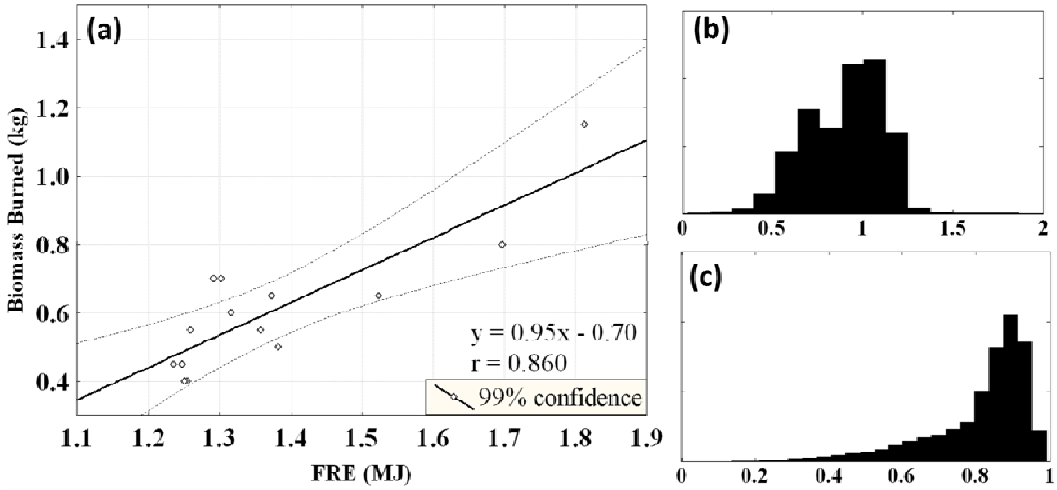

Figure 4. *Linear regression between the FRE and the total biomass consumed* ***(a)****; slope distributions* ***(b)*** *and correlation* ***(c)*** *using the bootstrap technique.*

3.2. Data assimilation and concentration results

Figure 5 shows the time series with near surface concentration of $PM_{2.5}$ (μg m^{-3}) and CO (ppb) estimated from biomass consumed coefficient assimilated in CCATT–BRAMS model (light grey) and observed data collected in LBA SMOCC/RaCCI (dark grey) in dry–to–wet Amazon transition season. During the CCATT–BRAMS simulation, three distinct regimes of rainfall could be observed in the Amazon basin. In the first weeks, a considerable number of vegetation fires are detected not only in the campaign area but all over the Amazon basin and Central Brazil due to low rainfall rates. The higher incidence of biomass burning in this period provides a strong variability in time series.

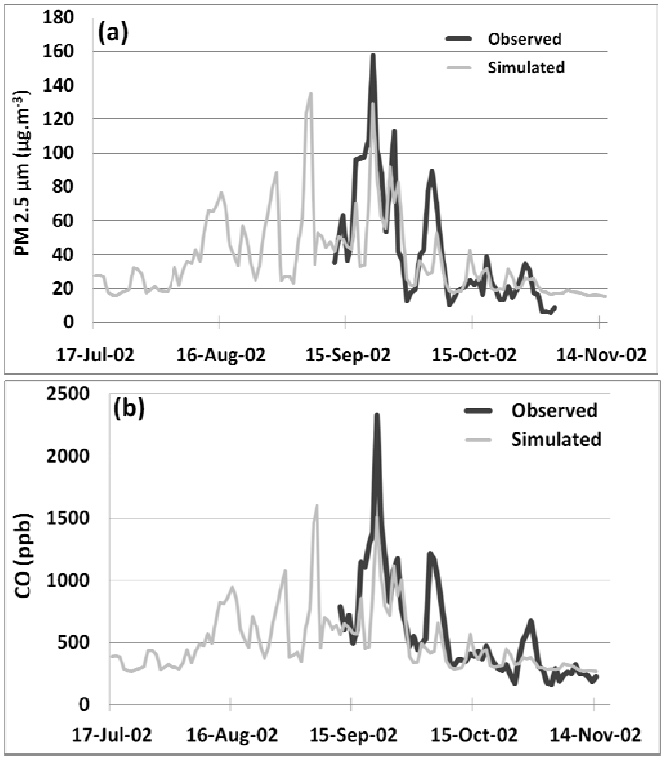

Figure 5. *Time series with near surface $PM_{2.5}$ (μg m^{-3}) observed (in dark grey) and estimated by the biomass burned coefficient (in light grey) in **(a)**; and CO (ppb) observed (in dark grey) and estimated by the biomass burned coefficient (in light grey) in **(b)**.*

In September, the surface $PM_{2.5}$ and CO measurements can reach approximately 160 μg m^{-3} and 2 400 ppb, respectively. Moreover, in October the rainfall rate begins to increase and, consequently, the number of vegetation fires decreases. In November the rainfall causes a notable decrease of fires, but a small number of hot spots are still observed. This reduction is evidenced when surface $PM_{2.5}$ and CO values are analyzed. As time series values are affected by the transport of burning biomass emissions that occurred in other regions, model time series results have shown a good agreement with observed data. In South America, the transport of aerosols and trace gases are commonly related with weather systems originated in the south of the continent.

To analyze CCATT–BRAMS model uncertainties, the bootstrap technique was used to calculate the correlation and slope confidence to CO and $PM_{2.5}$ simulations (Efron, 1982) and the Wavelet Transform (WT) with Morlet model of order 3 and global significance of 5% are used to analyze error variability (Mallat, 1989; Daubechies, 1992; Lindsay et al., 1996). Figure 6 shows the South America average concentration of $PM_{2.5}$ for CCATT–BRAMS simulations, between 17 July–14 November 2002, with FRP–based burned biomass coefficient in (a); the linear regression between Observed LBA SMOCC/RaCCI data (y–axis, in μg m^{-3}) and Modeled CCATT–BRAMS data (x–axis, in μg m^{-3}) with confidence interval (95%, in dashed line) in (b). Also, at the bottom of the regression graph, the confidence interval for correlation (c) and slope (d) are derived from bootstrap technique.

The highest concentration values of $PM_{2.5}$ are located in the "arc of deforestation" in northern Brazil. In this area, average concentration could reach values higher than 60 μg m^{-3}, with a diurnal daily emission exceeding 250 μg m^{-3} of $PM_{2.5}$. Moreover, CO concentrations for the same area might reached an average value greater than 700 ppb (Figure 7a), with a diurnal daily emission exceeding 2 500 ppb. Figure 7b shows the linear regression between observed data (y–axis, in ppb) and model results (x–axis, in ppb) with confidence interval of 95% (in dashed line). At the bottom of the regression graph, the confidence interval for correlation (c) and slope (d) are also derived from bootstrap technique.

The bootstrap frequencies for $PM_{2.5}$ and CO varied between 0.80 to 0.95 (significant at 0.01 level by student t–test) for both methods, with an average value centered at 0.95 (Figure 6c) and 0.92 (Figure 7c). Furthermore, the slope analysis reveals an underestimation of emission values with CCATT–BRAMS modeled values 20–30% lower than observed data. The underestimation occurs mainly on days with large fires. The $PM_{2.5}$ estimation shows overestimated values on days with low burning biomass observations such as in the November wet transition season and underestimated emissions in large fires.

To assess the model errors, relative to temporal variability of CO and $PM_{2.5}$ concentrations, the WT with Morlet model was applied to ground data observations and to model error estimates. The WT is a quantitative method to analyze time series by variances decomposition. It allows separating and recovering data in different time scales, in frequency domain, at which each scale is represented by a specific frequency (Torrence and Webster, 1999). One of the assumptions to perform the analysis by WT is a stationary pattern (the average should be constant throughout all data). To analyze the stationarity, the Lilliefors test was performed to verify if observed data and model error estimate time series have a normal distribution. In this case, the null hypothesis cannot be rejected at the 95% confidence level, thus there is no evidence to suppose that data did not have a normal distribution.

The WT analysis of ground measurements of CO and $PM_{2.5}$ concentrations showed a monthly variation (significant at 0.05 level by chi–square test). This is clearly reflected by gradual decrease of fire emissions in dry–to–wet Amazon transition season, since the highest emission values are found at the beginning of time series. However, model error estimate assessment reveals that the scale of variation of the phenomenon analyzed has a weekly variation on the first 10 days (significant at 0.05 level by chi–square test). During this period, the error associated with biomass burning emission estimation might reach approximately 30 μg m^{-3} and 330 ppb for $PM_{2.5}$ and CO, respectively.

This error source could be associated with some uncertainties in remote sensing derived products. Factors such as sensor channel saturation by high fire temperatures, undetected or missed fires, cloud cover, smoldering effects of fires in FRP estimation, regional characteristics of biomass burning and instantaneous fire size and temperature could contribute to emission underestimation (Pereira et al., 2009). On the other days of time series the variability behavior showed a monthly variation (significant at 0.05 level by chi–square test), related to fire emissions decrease, model performance and biomass burned coefficient efficiency to estimate emissions of low fires.

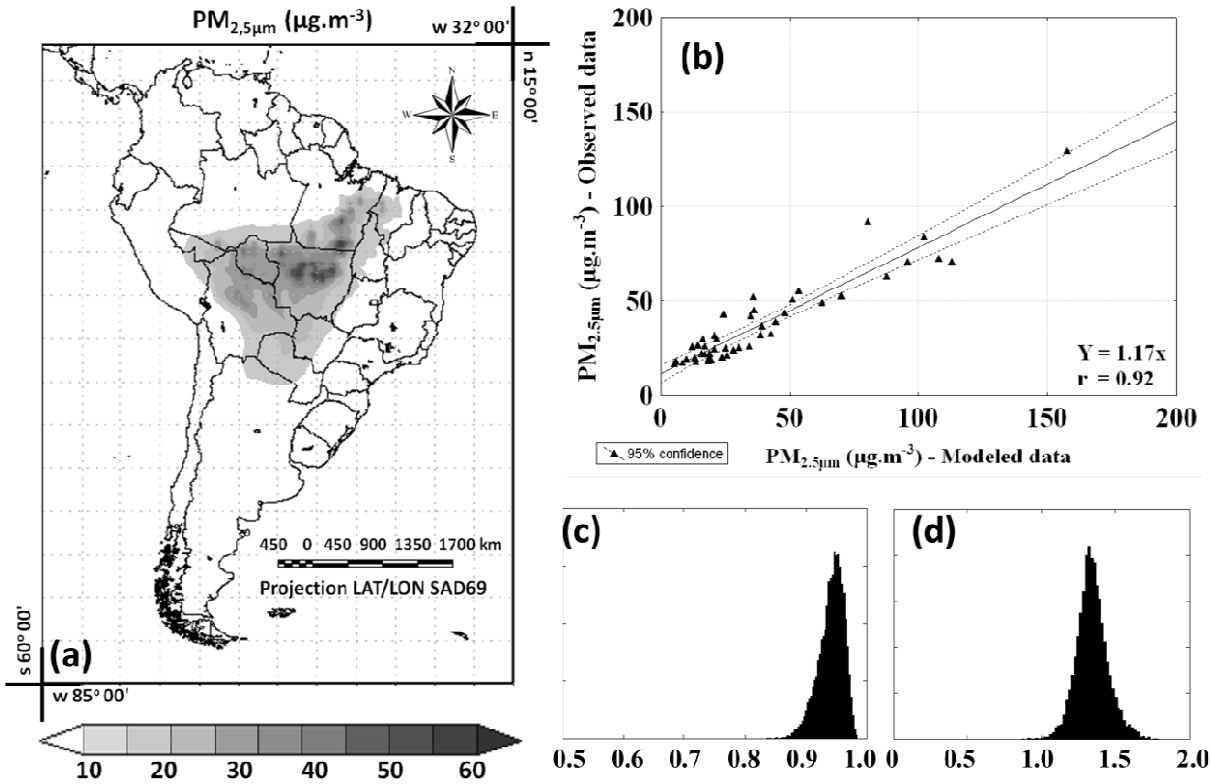

Figure 6. *Map with the average $PM_{2.5}$ released by biomass burning between 17 July 2002 and 14 November 2002* ***(a)****; linear regression between the modeled and the observed data* ***(b)****; bootstrap technique showing correlation* ***(c)*** *and slope* ***(d)*** *distributions.*

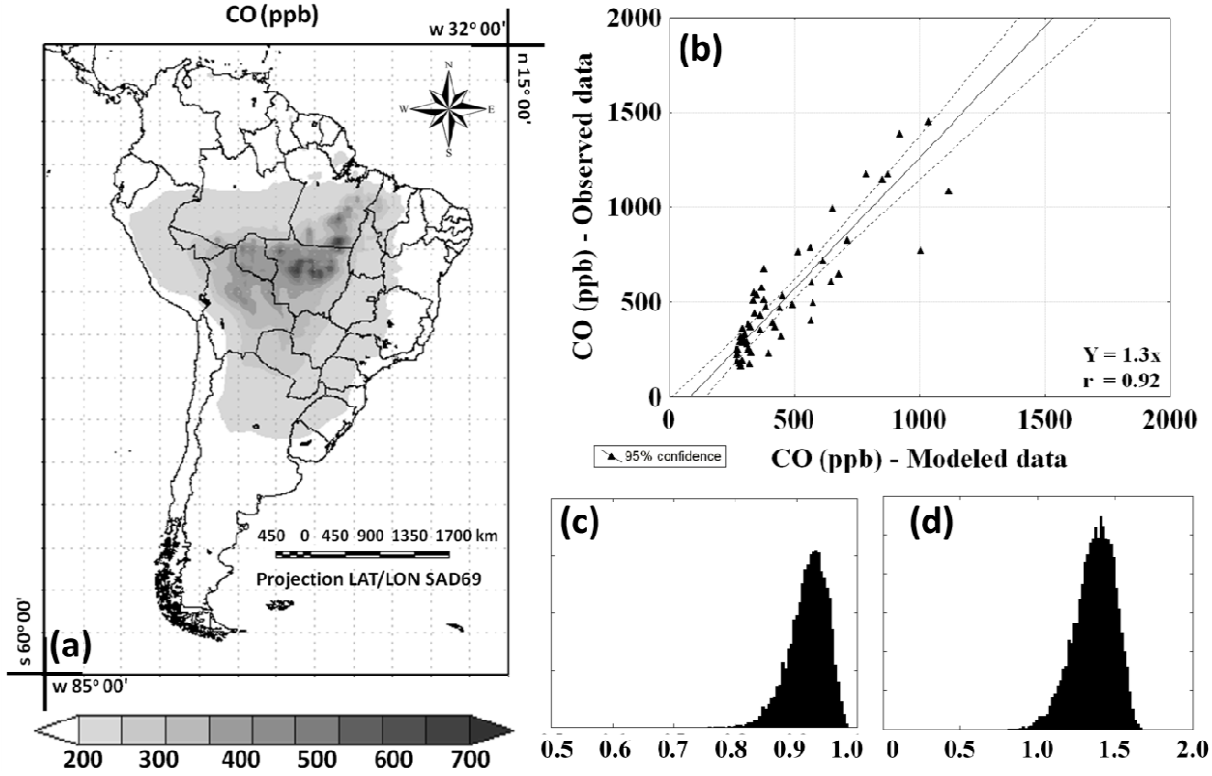

Figure 7. *Map with the average CO released by biomass burning between 17 July 2002 and 14 November 2002* ***(a)****; linear regression between the data modeled and the data observed* ***(b)****; bootstrap technique showing correlation* ***(c)*** *and slope* ***(d)*** *distributions.*

4. Conclusions

Estimates of biomass burning emissions are essential for annual inventories, therefore, data derived from environmental satellites are useful information for weather, climate and air quality models. The burned biomass coefficient derived by the relationship between the biomass consumed and FRE released rate show a good agreement with LBA SMOCC/RaCCI ground truth data and demonstrate a new methodology to trace gas and aerosol emissions. Nowadays, biomass burning emissions are estimated with emission factors. However, variables such as burned area, biomass density, fraction of the average above–ground burned biomass and the burn efficiency are hard to estimate and to use in near real–time air pollution forecast model applications.

In this work, relationship between the $PM_{2.5}$ and CO model shows a good agreement with SMOCC/RaCCI data in the general pattern of temporal evolution. The results showed high correlations between CCATT–BRAMS simulations with values between 0.80 and 0.95. Moreover, the slope analysis reveals an underestimation of 20–30% in emission values of 2002 South America dry season, observed mainly on days with large fires.

Although the coefficients of burned biomass suggest that the amount of biomass burned is proportional to FRE released, two additional experiments were conducted with different vegetation types and conditions. In spite of the fact that coefficient values seem to be different for each occasion, more experiments should be done with more vegetative species evaluating possible changes in their rates.

References

Andreae, M., Merlet, P., 2001. Emission of trace gases and aerosols from biomass burning. *Global Biogeochemical Cycles* 15, 955-966.

Andreae, M., Rosenfeld, D., Artaxo, P., Costa, A., Frank, G., Longo, K., Silva-Dias, M., 2004. Smoking rain clouds over the Amazon. *Science* 303, 1337-1342.

Biggar, S., Slater, P., Gellman, D., 1994. Uncertainties in the in-flight calibration of sensors with reference to measured ground sites in the 0.4-1.1 μg range. *Remote Sensing of Environment* 48, 245-252.

Chatfield, R.B., Guo, Z., Sachse, G.W., Blake, D.R., Blake, N.J., 2002. The subtropical global plume in the Pacific Exploratory Mission–Tropics A (PEM–Tropics A), PEM–Tropics B, and the Global Atmospheric Sampling Program (GASP): How tropical emissions affect the remote Pacific. *Journal of Geophysical Research* 107, art. no. 4278.

Christopher, S., Wang, M., Berendes, T., Welch, R., Yang, S., 1998. The 1985 biomass burning season in South America: satellite remote sensing of fires, smoke, and regional radiative energy budgets. *Journal of Applied Meteorology* 37, 661-678.

Chuvieco, E., Cocero, D., Aguado, I., Palacios, A., Prado, E., 2004. Improving burning efficiency estimates through satellite assessment of fuel moisture content. *Journal of Geophysical Research-Atmospheres* 109, art no. D14S07.

Crutzen, P., Andreae, M., 1990. Biomass burning in the tropics: impact on atmospheric chemistry and biogeochemical cycles. *Science* 250, 1669-1678.

Daubechies, I., 1992. *Ten lectures on wavelets*. 2ed, Vermont: Ed.City Press, 357p.

Dyominov, I., Zadorozhny, A., 2008. Greenhouse gases and future long-term changes in the stratospheric temperature and the ozone layer. *International Journal of Remote Sensing* 29, 2749-2774.

Efron, B., 1982. *The jackknife, the bootstrap, and other resampling plans*. Society of Industrial and Applied Mathematics, CBMS–NSF Monographs, 38.

Fearnside, P., Righi, C., Graca, P., Keizer, E., Cerri, C., Nogueira, E., Barbosa, R., 2009. Biomass and greenhouse-gas emissions from land-use change in Brazil's Amazonian "arc of deforestation": the states of Mato Grosso and Rondonia. *Forest Ecology and Management* 258, 1968-1978.

Fishman, J., Hoell, J., Bendura, R., McNeil, R., Kirchhoff, V., 1996. NASA GTE TRACE-A experiment (September October 1992). Overview. *Journal of Geophysical Research-Atmospheres* 101, 23865-23879.

Freeborn, P., Wooster, M., Hao, W., Ryan, C., Nordgren, B., Baker, S., Ichoku, C., 2008. Relationships between energy release, fuel mass loss, and trace gas and aerosol emissions during laboratory biomass fires. *Journal of Geophysical Research-Atmospheres* 113, art. no. D01102.

Freitas, S.R., Longo, K.D.M., Chatfield, R., Dias, P., Artaxo, P., Andreae, M., Grell, G., Rodrigues, L., Fazenda, A., Panetta, J., 2007. The Coupled Aerosol and Tracer Transport model to the Brazilian developments on the Regional Atmospheric Modeling System (CATT-BRAMS), Part 1: Model description and evaluation. *Atmospheric Chemistry and Physics Discussion* 7, 8525-8569.

Giglio, L., 2005. MODIS Collection 4 Active Fire Product User's Guide. Available on the Internet: http://maps.geog.umd.edu/products/MODIS_Fire_Users_Guide_2.1.pdf.

Horowitz, L., Walters, S., Mauzerall, D., Emmons, L., Rasch, P., Granier, C., Tie, X., Lamarque, J.F., Schultz, M., Brasseur, G., 2003. A global simulation of tropospheric ozone and related tracers: Description and evaluation of MOZART, version 2, *Journal of Geophysical Research* 108, art. no. 4784.

Ichoku, C., Kaufman, Y., 2005. A method to derive smoke emission rates from MODIS fire radiative energy measurements. *IEEE Transactions on Geoscience and Remote Sensing* 43, 2636-2649.

Justice, C., Giglio, L., Korontzi, S., Owens, J., Morisette, J., Roy, D., Descloitres, J., Alleaume, S., Petitcolin, F., Kaufman, Y., 2002. The MODIS fire products. *Remote Sensing of Environment* 83, 244-262.

Kaufman, Y., Justice, C., Flynn, L., Kendall, J., Prins, E., Giglio, L., Ward, D., Menzel, W., Setzer, A., 1998. Potential global fire monitoring from EOS-MODIS. *Journal of Geophysical Research-Atmospheres* 103, 32215-32238.

Kaufman, Y., Fraser, R., 1997. The effect of smoke particles on clouds and climate forcing. *Science* 277, 1636-1639.

Kaufman, Y.J., Remer, L.A., Ward, D.E., Kleidman, R., Flynn, L., Shelton, G., Ottmar, R.D., Li, R.R., Fraser, R.S., McDougal, D., 1996. Relationship between remotely sensed fire intensity and rate of emission of smoke: SCAR–C Experiment. *Global Biomass Burning,* J. Levin, Ed: The MIT Press, 685 – 696.

Kaufman, Y.J., Setzer, A., Ward, D., Tanre, D., Holben, B.N., Menzel, P., Pereira, M. C., Rasmussen, R., 1992. Biomass Burning Airborne and Spaceborne Experiment in the Amazonas (BASE–A). *Journal of Geophysical Research* 97, D13, 581–599.

Kaufman, Y., Tucker, C., Fung, I., 1990. Remote-sensing of biomass burning in the tropics. *Journal of Geophysical Research-Atmospheres* 95, 9927-9939.

Latifovic, R., Pouliot, D., 2007. Analysis of climate change impacts on lake ice phenology in Canada using the historical satellite data record. *Remote Sensing of Environment* 106, 492-507.

Liang, S., 2001. Narrowband to broadband conversions of land surface albedo I algorithms. *Remote Sensing of Environment* 76, 213-238.

Lindsay, R., Percival, D., Rothrock, D., 1996. The discrete wavelet transform and the scale analysis of the surface properties of sea ice. *IEEE Transactions on Geoscience and Remote Sensing* 34, 771-787.

Longo, K., Freitas, S.R., Setzer, A., Prins, E., Artaxo, P., Andreae, M., 2007. The Coupled Aerosol and Tracer Transport model to the Brazilian developments on the Regional Atmospheric Modeling System (CATT-BRAMS), Part 2: Model sensitivity to the biomass burning inventories. *Atmospheric Chemistry and Physics Discussion* 7, 8571-8595.

Mallat, S., 1989. A theory for multiresolution signal decomposition: the wavelet representation. *IEEE Transactions on Pattern Analysis and Machine Intelligence* 11, 674-693.

Moraes, E., Franchito, S., Rao, V., 2005. Evaluation of surface air temperature change due to the greenhouse gases increase with a statistical-dynamical model. *Journal of Geophysical Research-Atmospheres* 110, 1-8.

Nobre, C., Mattos, L., Dereczynski, C., Tarasova, T., Trosnikov, I., 1998. Overview of atmospheric conditions during the smoke, clouds, and Radiation - Brazil (SCAR-B) field experiment. *Journal of Geophysical Research-Atmospheres* 103, 31809-31820.

Panchenko, M., Sviridenkov, M., Terpugova, S., Kozlov, V., 2008. Active spectral nephelometry as a method for the study of submicron atmospheric aerosols. *International Journal of Remote Sensing* 29, 2567-2583.

Pereira, E., Martins, F., Abreu, S., Couto, P., Stuhlmann, R., Colle, S., 2000. Effects of burning of biomass on satellite estimations of solar irradiation in Brazil. *Solar Energy* 68, 91-107.

Pereira, G., Freitas, S., Moraes, E., Ferreira, N., Shimabukuro, Y., Rao, V., Longo, K., 2009. Estimating trace gas and aerosol emissions over South America: relationship between fire radiative energy released and aerosol optical depth observations. *Atmospheric Environment* 43, 6388-6397.

Reid, J., Eck, T., Christopher, S., Hobbs, P., Holben, B., 1999. Use of the angstrom exponent to estimate the variability of optical and physical properties of aging smoke particles in Brazil. *Journal of Geophysical Research-Atmospheres* 104, 27473-27489.

Roy, D., Lewis, P., Justice, C., 2002. Burned area mapping using multi-temporal moderate spatial resolution data a bi-directional reflectance model-based expectation approach. *Remote Sensing of Environment* 83, 263-286.

Satheesh, S., Moorthy, K., 2005. Radiative effects of natural aerosols: a review. *Atmospheric Environment* 39, 2089-2110.

Seinfeld, J., Pandis, S., 1998. *Atmospheric Chemistry and Physics*, John Wiley & Sons Inc., New York, 1309 pp.

Silva, J., Sa, A., Pereira, J., 2005. Comparison of burned area estimates derived from SPOT-VEGETATION and Landsat ETM+ data in Africa: influence of spatial pattern and vegetation type. *Remote Sensing of Environment* 96, 188-201.

Starks, P., Schiebe, F., Schalles, J., 1995. Characterization of the accuracy and precision of spectral measurements by a portable, silicon diode array spectrometer. *Photogrammetric Engineering and Remote Sensing* 61, 1239-1246.

Tarasova, T., Nobre, C., Eck, T., Holben, B., 2000. Modeling of gaseous, aerosol, and cloudiness effects on surface solar irradiance measured in Brazil's Amazonia 1992-1995. *Journal of Geophysical Research-Atmospheres* 105, 26961-26969.

Tzanis, C., Varotsos, C., 2008. Tropospheric aerosol forcing of climate: A case study for the greater area of Greece. *International Journal of Remote Sensing* 29, 2507-2517.

Torrence, C., Webster, P., 1999. Interdecadal changes in the ENSO–Monsoon system. *Journal of Climate* 12, 2679–2690.

van der Werf, G., Randerson, J., Giglio, L., Collatz, G., Kasibhatla, P., Arellano, A., 2006. Interannual variability in global biomass burning emissions from 1997 to 2004. *Atmospheric Chemistry and Physics* 6, 3423-3441.

Wagner, F., Muller, D., Ansmann, A., 2001. Comparison of the radiative impact of aerosols derived from vertically resolved (lidar) and vertically integrated (Sun photometer) measurements: example of an Indian aerosol plume. *Journal of Geophysical Research-Atmospheres* 106, 22861-22870.

Ward, D., Susott, R., Kauffman, J., Babbıtt, R., Cummings, D., Dias, B., Holben, B., Kaufman, Y., Rasmussen, R., Setzer, A., 1992. Smoke and fire characteristics for Cerrado and deforestation burns in Brazil: BASE-B Experiment. *Journal of Geophysical Research-Atmospheres* 97, 14601-14619.

Wooster, M., Roberts, G., Perry, G., Kaufman, Y., 2005. Retrieval of biomass combustion rates and totals from fire radiative power observations: FRP derivation and calibration relationships between biomass consumption and fire radiative energy release. *Journal of Geophysical Research-Atmospheres* 110, art. no., D24311.

Wooster, M., Zhukov, B., Oertel, D., 2003. Fire radiative energy for quantitative study of biomass burning: derivation from the bird experimental satellite and comparison to MODIS fire products. *Remote Sensing of Environment* 86, 83-107.

Wooster, M.J., 2002. Small–scale experimental testing of fire radiative energy for quantifying mass combusted in natural vegetation fires. *Geophysical Research Letters* 29, art. no., 2027.